

HIGH QUALITY SHIP HULL FORM REPRESENTATION BASED ON SUBDIVISION SURFACES

S H Greshake and R Bronsart, University of Rostock, Germany

SUMMARY

Usually, a hull form is represented by tensor-product spline surfaces. Due to the topological limitation of tensor-product splines to quadrilateral surfaces, hull forms are composed of several patches. This results in discontinuities of different order between neighboring patches. Indeed, this is known to be error-prone in practice. Furthermore, the quality of a hull surface measured in terms of fairness is limited due to discontinuities. Therefore, the goal of this work is to represent a hull form as single spline surface, which is the natural solution to avoid discontinuities.

Initially, subdivision surfaces are introduced. This is another mathematical approach to define tensor-product splines, but it allows for a generalization of spline surfaces to arbitrary topology. Afterwards, the hull form of a typical container vessel is represented by a single, generalized spline surface. The surface is basically curvature continuous (G^2) everywhere, which enables a high-quality representation of the hull form.

This document is formatted in the convention required for all conference papers

1. INTRODUCTION

The hull form is probably the most important information about a ship design. In general, the quality of a hull form is measured in terms of fairness. This quality criterion requires curvature continuity as well as a minimal number of inflection points. Naturally, it is the designer's responsibility to minimize the number of inflection points, though this task might be assisted by some fairing algorithm. In contrast, curvature continuity is a property of the geometric representation of the hull form.

Tensor-product spline surfaces are commonly used for hull form representation. In most cases cubic B-splines are employed. Indeed, a cubic B-spline offers the best trade-off between a minimal degree and curvature continuity. Unfortunately, tensor-product splines are limited to quadrilateral surfaces. Accordingly, a hull form is composed of several patches, but this results in discontinuities of different order between neighboring patches. In the context of the quality assessment of a hull surface, discontinuities are the major source of quality defects.

The worst case are discontinuities of zeroth order. In this case patches are disjoint and the hull form representation lacks any continuity across patch boundaries. Indeed, this does not only cause serious quality issues, but is also known to be error-prone in practice because disjoint patches limit the applicability of the hull form representation in downstream analysis methods. The possibility of disjoint patches may sound rather theoretical but they occur frequently in practice. Furthermore, substantial effort is required to prepare a hull form representation composed of disjoint patches for downstream applications, see for example the work of Bronsart et al. [1, 2, 3].

In contrast, high-order discontinuities essentially limit the quality of the hull surface representation. With respect to the quality criterion for hull forms, discontinuities of first and second order are of primary interest. Discontinuities of first order denote a lack of normal continuity across

patch boundaries. Similarly, discontinuities of second order indicate a lack of curvature continuity across patch boundaries. Usually, a hull form representation is generated based on a network of curves. The network is interpolated with appropriate surface patches that join smoothly. Most algorithms obtain normal continuity across patch boundaries [4]. In contrast, curvature continuity is necessary to meet the quality requirements defined above. Recall that in practice often neither normal nor position continuity is obtained, but disjoint patches are a daily occurrence.

Discontinuities between neighboring patches are identified as a major reason for quality defects of hull form representations based on tensor-product splines. Therefore the goal of this work is to represent a hull form as a single spline surface, which is the natural solution to avoid discontinuities.

In fact, the limitation of tensor-product splines to quadrilateral surfaces causes the necessity to compose a hull form of several patches. To negotiate this limitation, attention has to be paid to its reason. The reason is that tensor-product splines are defined on regular control meshes. In order to address this limitation, a possibility to define spline surfaces on arbitrary topological control meshes is required. Naturally, this leads to the idea of subdivision surfaces. A certain class of subdivision surfaces originates from the idea to generate B-spline surfaces on control meshes of arbitrary topology. Certainly, the most important example is the subdivision algorithm of Catmull and Clark [5], which generalizes cubic B-spline surfaces.

Subdivision surfaces have gained wide popularity in the field of animation movies. In this field they replaced tensor-product splines for the representation of complex objects. Nevertheless, in the field of engineering they are still rarely used for the representation of surfaces. This might originate from two complementary views on subdivision surfaces. On the one hand, subdivision is viewed as a refinement of a polyhedral mesh. This is satisfactory for rendering, but due to its discrete nature

unsatisfactory for engineering. Indispensable analytical properties, such as points on the surface, normals or curvature are not available exactly. On the other hand, subdivision surfaces can be viewed as spline surfaces with singularities at extraordinary knots. However, refinement allows to remove those singularities. This is the appropriate setup to evaluate analytical properties exactly and therefore suitable to meet engineering demands. This second approach to subdivision is still unusual, but recently featured in the monograph of Peters and Reif [6]. Subdivision surfaces are introduced in the first part of the article. The focus will be on the representation of B-spline surfaces based on subdivision. The mathematical details are minimized to a necessary extent, but the analytical nature of subdivision surfaces is emphasized. Afterwards, a subdivision algorithm that generalizes cubic B-spline surfaces is specified. Its application for the representation of a typical hull form is shown in the second part of the article.

2. SURFACE REPRESENTATION

2.1 SUBDIVISION SURFACES

The subsequent material is a brief description of the spline-based approach to subdivision surfaces featured by Peters and Reif [6].

A generalized spline surface is a continuous map

$$\mathbf{x}: \mathbf{S} \rightarrow \mathbb{R}^3 \quad (1)$$

where \mathbf{S} denotes the spline domain. The domain is composed of a set of indexed cells $\Sigma = [0,1]^2$. Note that cells are simply unit squares in \mathbb{R}^2 . For visualization purposes, the spline domain is embedded into the plane, though this may require to distort individual cells. As an example, the embedding of a spline domain composed of five cells is shown in the left part of Figure 1.

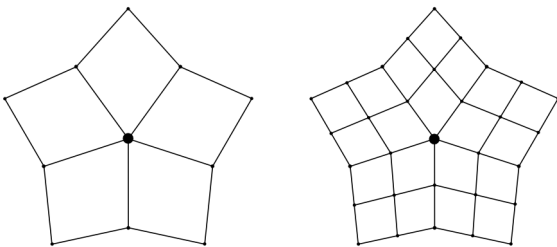


Figure 1: Embedding of a spline domain composed of five cells. The domain is divided by knots and knot lines. An extraordinary knot is highlighted in the center. Left: Initial domain. Right: Same domain after one step of refinement.

In analogy to the classical spline theory, the edges are called knot lines and meet at points called knots. Similar to a tensor-product spline the domain is divided by knots and knot lines. In contrast, extraordinary knots with $n \neq 4$ incident knot lines are allowed for generalized splines. An example of an extraordinary knot is highlighted in Figure 1. The restriction of the spline surface \mathbf{x} to a certain cell of its domain

$$\mathbf{x}_i: \Sigma \ni \sigma \mapsto \mathbf{x}(\sigma, i) \in \mathbb{R}^3 \quad (2)$$

is called a patch. Again, this is in compliance with the classical approach to spline surfaces, where complex surfaces are composed of several patches. However, those patches are now treated rigorously as a single surface, instead as a set of patches that might be interpreted as the representation of a single surface, but the patches are independent from a mathematical point of view.

Next, an expression for \mathbf{x} that maps any composed domain to a continuous surface in \mathbb{R}^3 is required. Unfortunately, no proper expression is known in the context of B-splines, though the restriction of \mathbf{x} to a patch \mathbf{x}_i can be easily defined in terms of tensor-product splines. For example:

$$\mathbf{x}_i(s, t) = \sum_{i=1}^4 \sum_{j=1}^4 b_i^3(s) b_j^3(t) \mathbf{q}_{ij} = B\mathbf{Q} \in \mathbb{R}^3 \quad (3)$$

is a cubic tensor-product B-spline surface on the unit square, where b_i^3 and b_j^3 are uniform cubic B-spline functions and \mathbf{q}_{ij} is a regular grid of 4×4 control points. This example is illustrated in the left part of Figure 2.

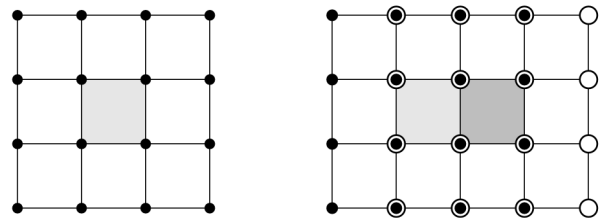


Figure 2: Connection of cubic spline patches with second-order continuity. Left: A single patch and its control mesh. Right: Smooth connection of two patches. Curvature continuity is provided because both patches share a part of their control meshes.

A simplified outline of the surface is shown in gray. The control mesh and the control points are shown in black. Furthermore, the right part of Figure 2 shows the connection of two patches with second order continuity. Apparently, second-order continuity is obtained because both patches share a proper set of control points. More patches could be connected, but the combined mesh would be always regular. Those composition of cubic patches to a smooth surface fits into the definition of a generalized spline, though irregular control meshes are disregarded. However, there is already an advantage over normal splines because the surface is not necessarily four-sided. Consider for example another patch on top of the dark gray patch in Figure 2. This would result in a L-shaped spline surface with six sides.

The key to irregular control meshes is subdivision. This term refers to a splitting of the spline domain. Every cell of the domain is split into four cells as shown in Figure 1. Recall that always one patch corresponds to one cell. Hence, the number of patches increases and therefore the number of control points increases, too. Indeed, the growing number of control points characterizes the first view on subdivision as a control mesh refinement. To obtain a new set of control points, the rules of knot insertion are employed. Hence, neither the shape of the

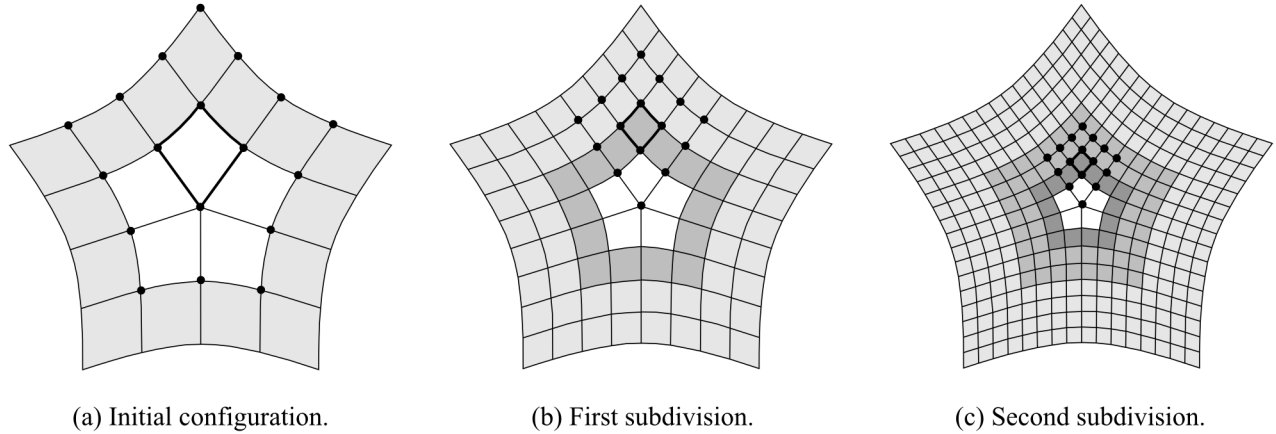


Figure 3: A generalized spline surface with an irregular control mesh. Patches incident to the extraordinary control point cannot be defined in terms of tensor-product splines. However, subdivision allows to add further rings of tensor-product spline patches in vicinity of the extraordinary point.

surface nor continuity properties change due to domain refinement. Naturally, knot insertion applies only for regular meshes, but because new control points are linear combinations of old control points, these rules can be generalized for irregular meshes. At the first glance, one could choose any rules for extraordinary control points. In fact, the rules for those points are constrained by continuity requirements.

Figure 3a shows a part of an irregular control mesh. For simplicity only a part of the mesh around the extraordinary point in the center is shown. The rest of the mesh is assumed to be regular. Therefore, the outer ring of patches is well defined in terms of cubic tensor-product splines. Furthermore, the patches are connected with second-order continuity because neighboring patches share control points as shown in Figure 2. In contrast, the inner patches do not possess any tensor-product representation due to the irregularity of the control mesh, see the control points highlighted in Figure 3a. One step of subdivision splits every patch into four patches and the control mesh is refined accordingly. This allows to add another ring of tensor-product splines in vicinity of the extraordinary point as shown in Figure 2b. It is easily verified that the new patches are connected with second-order continuity to its neighbors. A further step of subdivision adds a further ring of tensor-product splines, see Figure 3c. Thus, subdivision generates a growing tensor-product representation of the surface. Indeed, this is the appropriate setup to access analytical properties of a generalized spline exactly, even in the presence of extraordinary points. The next paragraph makes this approach to subdivision precise.

Recall the matrix notation of single spline patch in equation (3). Furthermore, let m denote the number of subdivision steps applied in the vicinity of the extraordinary point. Then

$$\mathbf{x}_i^m = B \mathbf{Q}_i^m \quad (4)$$

is the i -th patch of the m -th ring, where B contains the B-spline functions and \mathbf{Q}_i^m contains the corresponding control points. Apparently, B is invariant to subdivision, but \mathbf{Q}_i^m is a subset of the control mesh that changes every

step. Next, all patches of the m -th ring are composed to single expression

$$\mathbf{x}^m = G \mathbf{Q}^m \quad (5)$$

where G is called a system of generating rings and can be thought as an appropriate arrangement of B-spline functions that results from the composition of B . However, \mathbf{Q}^m is still undefined. Recall that a new set of control points results from a simple linear combination of old control points that can be expressed in matrix notation. This allows to define, the control points of the m -th ring

$$\mathbf{Q}^m = A^m \mathbf{Q} \quad (6)$$

directly in terms of the initial control points \mathbf{Q} . The coefficients of the linear combination are encoded in the subdivision matrix A . Now, the mathematical setting enables the analytical expression of every spline ring

$$\mathbf{x}^m = G A^m \mathbf{Q} \quad (7)$$

in terms of the initial data \mathbf{Q} . Furthermore, the limit

$$\mathbf{x}^c = \lim_{m \rightarrow \infty} G A^m \mathbf{Q} \quad (8)$$

defines the central point.

In summary, subdivision generates a tensor-product representation of a generalized spline surface in the presence of extraordinary points. With equation (7) and equation (8) an expression to access those representation immediately in terms of the initial control mesh \mathbf{Q} is given. In fact, this expression is only slightly more complex than the definition of tensor-product splines given in equation (3), but requires to exponentiate the matrix A . This can be done very efficiently, replacing A with its spectral decomposition.

The generalized spline surface inherits its continuity properties from the spline functions, except at extraordinary points. Recall, that in case of cubic B-spline functions all patches generated by subdivision are connected with second-order continuity. However, to analyze continuity properties at the central point is much more difficult. In fact, the major task to construct a subdivision surface is to define refinement rules for the extraordinary points that guarantee continuity at the central point.

2.2 SUBDIVISION ALGORITHM

Subdivision is a method to generate a tensor-product representation of a generalized spline surface in the vicinity of extraordinary knots. This method is put into operation by the tuple (A, G) , which is called the subdivision algorithm. In fact, both components form a unit because A results from the generalization of knot insertion of the spline functions that identify G .

In this article, the subdivision algorithm of Catmull and Clark [5] is used. The algorithm is a generalization of knot insertion for uniform cubic tensor-product B-splines. In addition, the surface may contain creases and corners as features. This is realized with a subset of the extensions proposed by Biermann et al. [7]. In general, the surface is curvature continuous (G^2) everywhere, but at extraordinary points it is only normal continuous (G^1).

2.2 (a) Feature definition

Features of the surface are defined based on tags applied to the control mesh. However, the choice of tags may be interdependent.

Edge tags: Edges of the control mesh can be tagged to be smooth or crease. By default, edges are smooth, except for boundary edges that are always creases.

Vertex tags: By default, vertices are smooth. Vertices incident to exactly two crease edges must be either tagged as a crease vertex or as a corner vertex. Vertices incident to a single crease edge are tagged as a dart vertex. Vertices incident to three or more crease edges are always tagged as corner vertices.

2.2 (b) Control points

Every subdivision step results in a new control mesh. Therefore, a new set of control points is computed. The presentation of the rules for new control points is based on the article of Biermann et al. [5], but all rules are generalized for non-quad meshes. However, these generalizations reproduce the original rules in case of a quad mesh. Furthermore, these rules include the original rules of Catmull and Clark [5].

Face points: For each face of the control mesh a new control point

$$\mathbf{f}_i = \frac{1}{n} \sum_{i=1}^n \mathbf{p}_i \quad (9)$$

is computed as the average of the n vertices \mathbf{p}_i defining the face.

Edge points: For each smooth edge of the control mesh a new control point

$$\mathbf{e}_i = w_1 \mathbf{p}_1 + w_2 \mathbf{p}_2 + \frac{1}{4} (\mathbf{f}_1 + \mathbf{f}_2) \quad (10)$$

is computed as the weighted average of the vertices \mathbf{p}_1 and \mathbf{p}_2 defining the edge and the face points \mathbf{f}_1 and \mathbf{f}_2 of the two faces incident to the edge. The choice of weights w_1 and w_2 depends on the tags of \mathbf{p}_1 and \mathbf{p}_2 .

If both vertices are (not) smooth the weights are simply $w_1 = w_2 = 1/4$. If one vertex is smooth and the other

vertex is not smooth, the weights are parametrized by θ_k where k is the number of faces in the sector of the edge. The notion of a sector is illustrated in Figure 4.

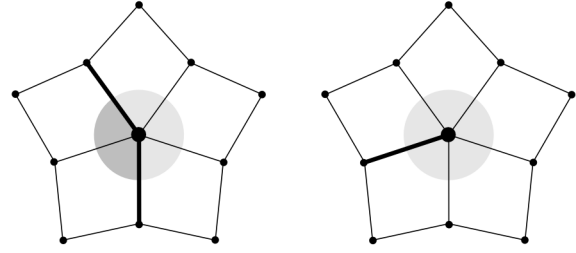


Figure 4: Crease edges of the control mesh are shown in bold and divide the mesh around the central vertex into sectors. Left: The mesh is divided into a sector of two faces and a sector of three faces. Right: A single sector of five faces.

Given the definition of a sector, the weight of the non-smooth vertex is

$$w = \frac{1}{2} \cos^2(\theta_k) \quad (11)$$

and the weight of the smooth vertex is

$$w = \frac{1}{2} \sin^2(\theta_k) \quad (12)$$

with $\theta_k = \pi/(4k)$ for a corner vertex, $\theta_k = \pi/(2k)$ for a crease vertex and $\theta_k = \pi/k$ for a dart vertex. The definition of θ_k for corner vertices is slightly modified in comparison to the original rules of Biermann et al. [7].

For each crease edge of the control mesh a new control point

$$\mathbf{e}_i = \frac{1}{2} \mathbf{p}_1 + \frac{1}{2} \mathbf{p}_2 \quad (13)$$

is computed as the average of the vertices \mathbf{p}_1 and \mathbf{p}_2 defining the edge.

Vertex points: The rule for a new vertex point depends on the tag of the vertex. For each smooth or dart vertex of the control mesh a new control point is defined by

$$\mathbf{v}_i = \frac{1}{n} \sum_{i=1}^n \mathbf{f}_i + \frac{1}{2n} \sum_{i=1}^n (\mathbf{p}_c + \mathbf{p}_i) + \frac{n-3}{n} \mathbf{p}_c \quad (14)$$

with \mathbf{f}_i are the face points of the faces incident to the vertex, \mathbf{p}_i are the surrounding vertices and \mathbf{p}_c is the position of the old vertex. For each crease vertex a new control point

$$\mathbf{v}_i = \frac{1}{8} \mathbf{p}_1 + \frac{3}{4} \mathbf{p}_c + \frac{1}{8} \mathbf{p}_2 \quad (15)$$

is computed as the weighted average of the adjacent crease vertices \mathbf{p}_1 , \mathbf{p}_2 and the position of the old vertex \mathbf{p}_c . For each corner vertex a new control point is simply given by $\mathbf{v}_i = \mathbf{p}_c$.

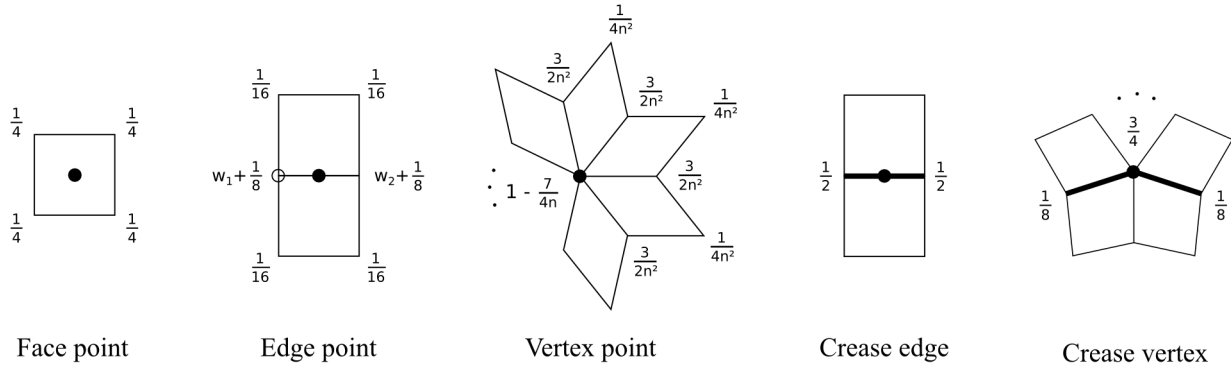


Figure 5: Stencils for the subdivision algorithm. A stencil represents a row the subdivision matrix A after the first step of subdivision. From left to right: Stencil of a face point (9), a smooth edge point (10), a smooth or dart vertex point (14), a crease edge (13) and a crease vertex (15).

2.2 (c) Subdivision matrix

After the first step of subdivision all faces of the control mesh are quadrilateral. Furthermore, the local topology around any point of the control mesh does not change with further steps of subdivision. Indeed, this is the right setup to specify the subdivision matrix A explicitly. Recall that A maps a set of control points \mathbf{Q}^m that defines a ring of tensor-product patches \mathbf{x}^m in vicinity of some extraordinary point to a new set of control points \mathbf{Q}^{m+1} that defines a further ring of patches \mathbf{x}^{m+1} . Naturally, the rules presented in section 2.2 (b) are used for this operation. Because those rules apply weighted averaging to obtain new control points, they can be rewritten in matrix notation

$$\mathbf{Q}^{m+1} = A\mathbf{Q}^m \quad (16)$$

where every row of the subdivision matrix A contains the weights of a single rule. The rows of A are given in terms of the stencils shown in Figure 5. In contrast to the equations given in section 2.2 (b), the stencils are only valid for purely quad meshes.

2.2 (d) Example

The capabilities of the subdivision algorithm described in this section are illustrated in Figure 6. As an example, a five-sided surface is constructed. The control mesh of the surface is shown in the left part of Figure 6. In general, bold edges identify crease edges. As declared in section 2.2 (a), all boundary edges are required to be creases. In addition, one interior edge is tagged as a crease, too. Furthermore, the whole range of vertex tags is applied to the control mesh. Filled circles indicate corner vertices and empty circles denote crease vertices. The center vertex is a dart vertex because it is incident to a single crease edge.

The corresponding surface of this control mesh is shown in the right part of Figure 6. Now, the tags can be discussed in terms of surface features. A chain of crease edges forms a control polygon of a cubic spline curve. This curve is interpolated by the surface. Thus, to require all boundary edges to be creases yields a behavior of the surface similar to tensor-product splines with open knots vectors. In

addition, the corner vertices introduce cusps to the boundary curve. Again, this behavior is similar to the effect of multiple knots in classical spline theory. Naturally, the same characteristics apply for interior creases, but the surface is only position continuous (G^0) at those curves. Finally, a dart vertex causes an interior crease to fade out smoothly, as shown in the center of Figure 6.

Although this example is quite simple, it shows the full range of capabilities of the surface representation, most notably the definition of a multi-sided surface with an irregular control mesh. The boundary behavior of the surface is similar to that of open tensor-product splines. The definition of surface features is carried out with tags applied to the control mesh, rather than to modify knot vectors.

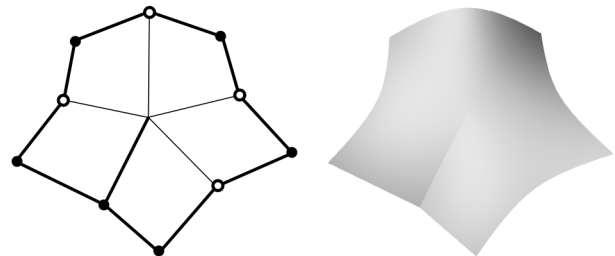


Figure 6: A simple five-sided surface. Left: The control mesh with crease edges (bold edges), corner vertices (black circles), crease vertices (empty circles) and a dart vertex in the center. Right: The corresponding surface with an interior crease that fades out at the dart vertex.

3. CASE STUDY

In this section, the surface representation described in section 2.2 is employed to represent the hull form of a modern container vessel. The hull form of the Duisburg Test Case (DTC) is considered as reference. The reference character of this hull form is twofold. Firstly, its design represents the hull form of typical modern container vessels, see [8]. Therefore, the applicability of the surface representation proposed in this article is measured against actual industry demands. Secondly, the geometric representation of the DTC fits into the common practice

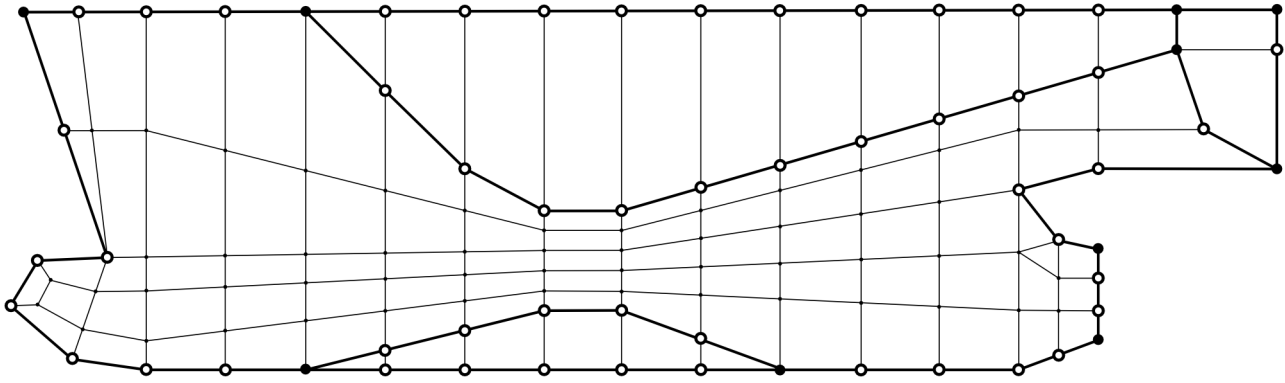


Figure 7: Chart of the control mesh used to define the hull form of a modern container vessel. The mesh consists of 117 control points. The boundary, the flat of side, the flat of bottom and the flat transom are modeled with crease edges (bold edges) in conjunction with crease vertices (empty circles) and corner vertices (black circles). All other vertices and edges are smooth.

for hull form representation. The hull form is provided as a set of cubic tensor-product B-spline patches, whereby an irregular network of curves is used for creation. In general, the patches meet with normal continuity, but in the forebody patches that meet only with position continuity are observed, too. However, the notion of continuity does not apply precisely, but within small tolerances. It is unclear whether this results from data exchange or is a deficiency of the method used for curve interpolation.

The hull form representation of the DTC is shown in Figure 8. It includes a flat transom and is composed of 660 patches. This number does not result from the topological limitation of tensor-product splines to quadrilateral surfaces, but from the complexity of the curve network used for surface generation. In general, it is possible to represent the hull form of typical container vessels with a smaller number of patches. In practice, at least a few tens of patches are required. Figure 9 shows the hull form of a container vessel represented based on subdivision surfaces. The hull form is similar to that of the DTC and is entirely represented with a single surface. In particular, this includes common features of the hull form such as the flat transom as shown in the right part of Figure 9.

3.1 CONTROL MESH

A chart of the control mesh used to define the hull form of a container vessel based on subdivision surfaces is shown in Figure 7. The control mesh consists of 117 control points. Most control points are organized in sections. Crease edges are used to separate certain regions of the hull form, namely the flat of side, the flat of bottom and the flat transom.

3.1 (a) Bulbous bow

The representation of a bulbous bow is challenging in case of tensor-product splines. From a geometric point of view, the bulbous bow is a two-sided surface, whereas tensor-product splines are always four-sided. One solution is to compose the bulbous bow of multiple patches, whereby at least two patches are degenerated. An example of this

solution is shown in Figure 8. In contrast, Figure 7 shows the representation of a bulbous bow based on an irregular control mesh. Two interior control points of valence three enable the typical shape of the bulbous bow. An extraordinary boundary control point of valence five is necessary to join it to the rest of the forebody.

3.1 (b) Flat of side

A chain of crease edges is used to define the flat of side as shown in Figure 7. In general, this yields a knuckle on the hull form. Though a knuckle is likely to be used as a flat of side above the design waterline, normal continuity is required in vicinity or below the design waterline. To force normal continuity, smooth edges incident to the flat of side are in the same plane. However, this does not force curvature continuity. At corners normal continuity is provided when all crease edges are in the same plane. For the corner vertex that joins the flat of side with the deck this criterion does not hold. Therefore, the flat of side is a knuckle close to the deck that fades out quickly as shown in Figure 9.

3.1 (c) Flat of bottom

The flat of bottom is realized similar to the flat of side. Again, crease edges are used for definition. In addition, normal continuity is forced at both corners. Hence, the flat of bottom is normal continuous everywhere.

3.1 (d) Flat transom

To incorporate the flat transom, crease edges are defined as shown in Figure 7. In contrast to the flat of side and flat of bottom, no normal continuity is forced. Therefore, the creases result in a knuckle as shown in Figure 9.

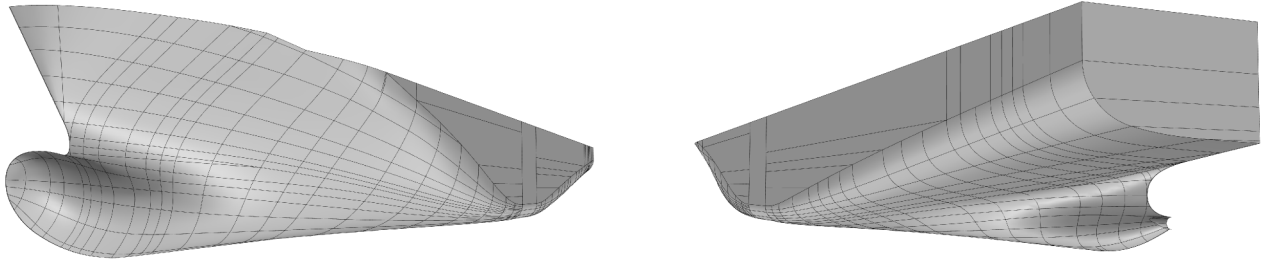


Figure 8: Hull form representation of the Duisburg Test Case (DTC) based on tensor-product splines. It is composed of 660 patches. Patch boundaries are shown as black curves.

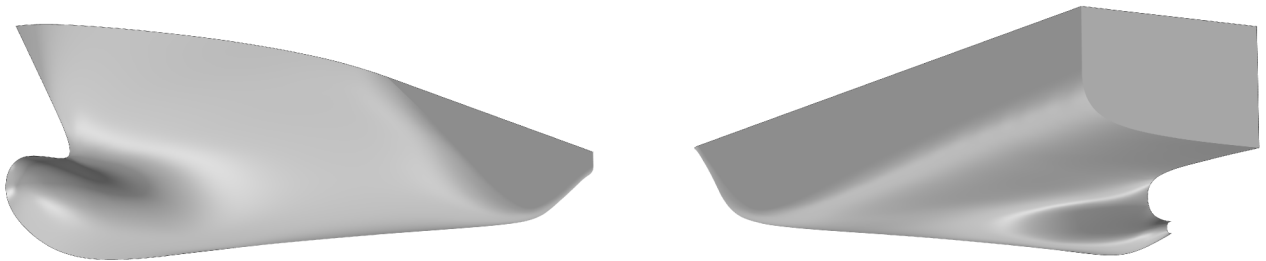


Figure 9: Hull form of a modern container vessel represented by a subdivision surface. The hull form is entirely represented by a single surface and includes common features such as the flat transom.

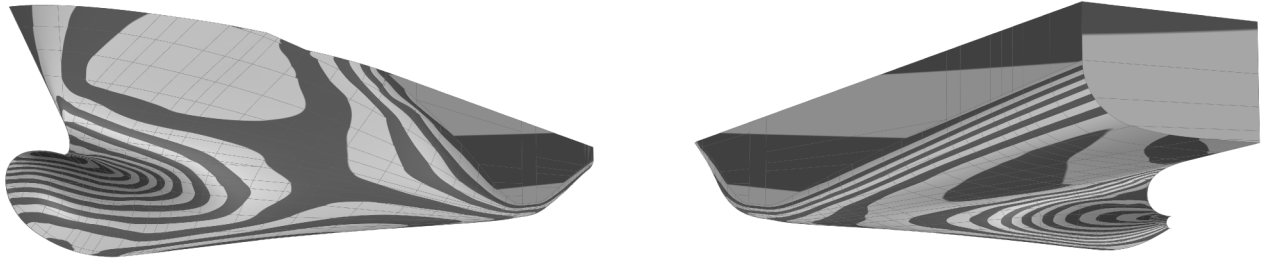


Figure 10: Reflection analysis of the DTC. The reflection lines show a lack of curvature continuity at patch boundaries. At some boundaries of the forebody, an additional lack of normal continuity is shown.

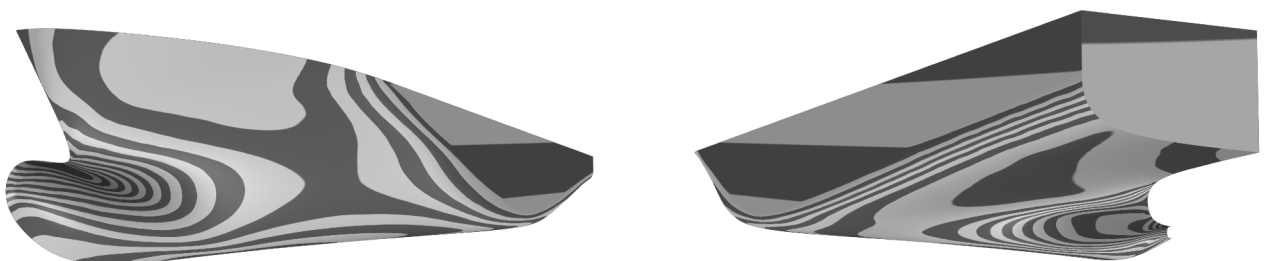


Figure 11: Reflection analysis of the subdivision surface. The reflection lines indicate curvature continuity everywhere. However, the definition of features such as the flat transom or the flat of side enables intended discontinuities.

3.2 ANALYSIS

Reflection lines are employed to analyze continuity properties. Curvature continuity is required for a high-quality hull form representation. Therefore, the best case are smooth reflection lines. Second order discontinuities are shown with a kink in reflection lines. In this case, there is a lack of curvature continuity at the kink, but normals are continuous. First order discontinuities are shown with disjoint reflection lines. A lack of both, curvature and normal continuity, is shown at those points.

3.2 (a) Global analysis

Figure 10 shows the reflection analysis of the DTC. In general, the reflection lines denote a lack of curvature continuity at patch boundaries. Furthermore, a lack of normal continuity is observed in some regions of the forebody. Certainly, the angular errors of normals are small because the reflection lines are disjoint but close to each other.

Figure 11 shows the reflection analysis of the subdivision surface. As expected, the reflection lines are smooth what denotes curvature continuity. The global pattern of the reflection lines agrees with the DTC. However, the absence of discontinuities avoids local oscillations of the reflection lines.

3.2 (b) Local analysis

To maintain continuity between adjacent tensor-product patches is particularly difficult in complex shaped regions of the hull form. As an example of a complex shaped region, Figure 12 shows a part of the bulbous bow.

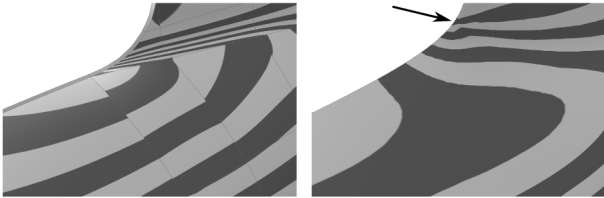


Figure 12: Reflection analysis of a part of the bulbous bow. Left: Reflection lines of the DTC show a serious lack of normal and curvature continuity across patch boundaries. Right: Reflection lines of the subdivision surface denote curvature continuity. The arrow points to an extraordinary point on the surface that causes a local distortion of the reflection lines.

The representation based on tensor-product splines shows serious discontinuities between neighboring patches. Reflection lines have notable kinks or even do not match. Those quality defects cause a significant limitation of surface quality. In contrast, the reflection lines of the subdivision surface are smooth. However, extraordinary points are required to model this region. The arrow shown in Figure 12 points to an extraordinary point. It causes a local distortion of the reflection lines. This is a well-known limitation of subdivision surfaces.

4. CONCLUSIONS

The impact of high-order discontinuities on the quality of a hull form representation seems to be negligible at the first glance. However, the comparison of the reflection lines of a hull form that merely lacks curvature continuity on the patch boundaries with its curvature continuous counterpart reveals a significant difference of quality. Indeed, this justifies to require curvature continuity for a high-quality hull form representation. In fact, this insight comes as no surprise because the well-established fairing of ship lines with a spline implies curvature continuity, too.

To require curvature continuity for a high-quality hull form representation is in conflict with the limitation of tensor-product splines to quadrilateral surfaces. As a consequence of this limitation, a hull form is composed of several patches, but discontinuities of different order are commonly observed on patch boundaries. On the other hand, subdivision surfaces allow a curvature continuous representation of hull forms. Furthermore, they are closely related to tensor-product splines. Essentially, subdivision is introduced as a method to generate a tensor-product representation of a subdivision surface. Therefore, subdivision surfaces are proposed to replace classical tensor-product splines for hull form representation.

The subdivision algorithm presented in this article is successfully used to represent the hull form of a modern container vessel. However, the focus of this study is the quality improvement of hull form representation based on subdivision surfaces, but not to provide a general purpose subdivision algorithm for hull form design. Future work will systematically focus on features the hull form representation should provide in order to support hull form modeling and how to realize those features based on subdivision.

5. REFERENCES

1. BRONSART, R., EDESSA, D. M., KLEINSORGE, L., 'Assuring Quality in Hull Form Representations for Downstream Applications', *Proceedings of 2nd International Conference on Maritime Engineering*, 2014.
2. BRONSART, R., EDESSA, D. M., KLEINSORGE, L., 'Automatic Pre-Mesh CAD Data Repairing', *International Journal of Mechanical Engineering and Applications*, 2013.
3. BRONSART, R., EDESSA, D. M., KLEINSORGE, L., 'A Contribution to Automatic Ship Hull Form CAD Data Repairing', *12th International Symposium on Practical Design of Ships and Other Floating Structures*, 2013.
4. NOWACKI, H., BLOOR, M. I. G., OLEKSIEWICZ, B., 'Computational Geometry for Ships', *World Scientific*, 1995.

5. CATMULL, E., CLARK, J., 'Recursively generated B-spline surfaces on arbitrary topological meshes', *Computer-Aided Design* 10 (6), 1978.
6. PETERS, J., REIF, U., 'Subdivision Surfaces', *Springer*, 2008.
7. BIERMANN, H., LEVIN, A. ZORIN, D., 'Piecewise smooth subdivision with normal control', *Proceedings of the ACM SIGGRAPH Conference on Computer Graphics*, 2000.
8. EL MOCTAR, O., SHIGUNOV, V., ZORN, T., 'Duisburg Test Case: Post-Panamax Container Ship for Benchmarking', *Ship Technology Research*, 59 (3), 2012.

9. AUTHORS BIOGRAPHY

Robert Bronsart is holding the Chair of Naval Architecture at the Department of Mechanical Engineering and Marine Technology at the University of Rostock. He has more than 30 years experience in R&D in ship design, production and operation, thereof ten years in industry. In research he is focusing on information and communication systems in collaboration networks, CAE-system integration and on knowledge based methods in ship design and operation. He is head of a research group with an interdisciplinary background performing research in cooperation with many partners from the German and European maritime industry.

Sebastian Greshake is a research assistant at the Chair of Naval Architecture at the University of Rostock. His research focuses on the application of subdivision surfaces for hull form representation. He graduated from the University of Rostock with a Master's degree in Naval Architecture and Ocean Engineering. Previously, he completed a cooperative engineering studies program with a Bachelor's degree in Mechanical Engineering at the Hochschule Niederrhein, University of Applied Sciences. The practical training included several internships as well as a vocational training and took place at Siemens.